

Quality evaluation of spaceborne SiC mirrors (II): evaluation technology for mirror accuracy using actual measurement data of samples cut out from a mirror surface

Masaki Kotani,^{1,*} Tadashi Imai,² Haruyoshi Katayama,² Yukari Yui,² Yoshio Tange,²
Hidehiro Kaneda,³ Takao Nakagawa,⁴ and Keigo Enya⁴

¹Aerospace Research and Development Directorate, Japan Aerospace Exploration Agency,
6-13-1 Ohsawa, Mitaka-shi, Tokyo 181-0015, Japan

²Space Applications Mission Directorate, Japan Aerospace Exploration Agency, 2-1-1 Sengen,
Tsukuba-shi, Ibaraki 305-8505, Japan

³Graduate School of Science, Nagoya University, Furo-cho, Chikusa-ku, Nagoya-shi, Aichi 464-8602, Japan

⁴Institute of Space & Astronautical Science, Japan Aerospace Exploration Agency, 3-1-1 Yoshinodai,
Chuo-ku, Sagami-hara-shi, Kanagawa 252-5210, Japan

*Corresponding author: kotani.masaki@jaxa.jp

Received 20 June 2013; revised 5 August 2013; accepted 6 August 2013;
posted 7 August 2013 (Doc. ID 192643); published 3 September 2013

The authors studied the quality evaluation technology of a spaceborne large-scale lightweight mirror that was made of silicon carbide (SiC)-based material. To correlate the material property of a mirror body and the mirror accuracy, the authors evaluated the mirror surface deviation of a prototype mirror by inputting actually measured coefficient of thermal expansion (CTE) data into a finite element analysis model. The CTE data were obtained by thermodilatometry using a commercial grade thermal dilatometer for the samples cut from all over the mirror surface. The computationally simulated contour diagrams well reproduced the mirror accuracy profile that the actual mirror showed in cryogenic testing. Density data were also useful for evaluating the mirror surface deviation because they had a close relationship with the CTE. © 2013 Optical Society of America

OCIS codes: (160.4670) Optical materials; (220.4840) Testing; (240.6700) Surfaces; (350.4600) Optical engineering; (350.6090) Space optics.

<http://dx.doi.org/10.1364/AO.52.006458>

1. Introduction

One of the most important requirements for improving the observation performance of reflecting telescope systems onboard space telescopes is an increase in the aperture of the primary mirror [1,2].

A key challenge in increasing the aperture is the reduction of the area density of the mirror body for the launch and ground testing. The use of silicon carbide (SiC), which has a superior specific modulus of elasticity and specific thermal diffusivity, is attracting attention as a method to drastically reduce the area density [3,4]. However, the coefficient of thermal expansion (CTE) of SiC materials is an order of magnitude greater than that of glass materials, and

hence, the risk of degrading the optical performance by thermal deformation of the mirror surface increases. Although there has been considerable improvement, the variation in quality within, and between, components still tends to increase as the manufacturing scale increases. Therefore, in order to increase the aperture of a spaceborne SiC mirror, appropriate quality control for suppressing property variation and improving reproducibility of manufacturing becomes increasingly important.

In this study, in an effort to establish a technique for evaluating the quality of the SiC mirror body, we investigated a basic technology for evaluating mirror accuracy based on property variation. We conducted thermal-structural analysis using the finite element method (FEM) and inputting experimentally obtained CTE data from the sample pieces cut out from various parts of a prototype mirror body surface. With this technology, we can perform a quality evaluation by simply testing sample pieces and analyzing the results on a computer, without mirror surface finishing or testing, which is generally time consuming and costly. This technology will allow us to screen and improve the processing of mirror materials. Considering practical utility in the mirror body development, we obtained material property data by using commercially available equipment and preparing samples of necessary dimensions. We verified the effectiveness of the evaluation by comparing the deviation profile of the entire mirror surface from the ideal one, as simulated through the computational analysis, with the profile obtained by cryogenic mirror surface testing.

One of the noticeable features is whether we can conduct a useful evaluation of the mirror accuracy with the measurement accuracy of CTEs obtained using a commercially available thermodilatometer for the samples cut out at 30 mm intervals. The intervals of 30 mm are the minimum dimensions to make necessary samples. In addition, making a disc-shaped product, such as a mirror, by using a manufacturing method that uses powders as raw materials, such as the reaction sintering method, involves many processes in which the forces act in the radial direction, such as the flow of slurry while making a compact or the heat transmission during sintering. Therefore, nonuniformity may arise between the surface in the circumferential direction and that in the radial direction. Hence, we cut out samples at various locations along the mirror surface both in the circumferential direction and in the radial direction, and examined the effect of such processes on the accuracy of mirror surface evaluation when considering the directionality of the sample pieces in the analysis. We also examined the effect of a variation in the behavior of the CTE according to the temperature caused by the nonuniformity of materials. Furthermore, we examined the practicality of mirror surface evaluation using the density data, which can be measured in a considerably shorter time than CTE measurements.

In order to effectively evaluate mirror accuracy based on CTE variation, the measurement error must be sufficiently small with respect to the CTE variation within the mirror body. Based on the result of the previous case study [5], we can expect a deviation of about 100 nm per 1% variation of the CTE between the regions inside and outside the circular area with a nominal radius of about 15 mm, when the entire mirror body with a base CTE of $2.4 \times 10^{-6}/\text{K}$ is uniformly cooled down by 200 K. Because the mirror surface usually requires an accuracy of 1/10 or less of the wavelength being observed, in the case of observation by visible light where the wavelength range is between 400 and 800 nm, the deviation value of 100 nm serves as a prerequisite guideline. Since 1% of $2.4 \times 10^{-6}/\text{K}$ is $0.024 \times 10^{-6}/\text{K}$, an accuracy level of almost $10^{-8}/\text{K}$ is needed for a suitable measurement accuracy of the CTE.

2. Experimental Methods

A. Mirror Body to Be Evaluated

A prototype spherical mirror, as shown in Fig. 1, was used as a model mirror body for evaluating the typical trends in changes in mirror accuracy due to thermal deformation. It was made entirely of SiC, with an outer diameter of 160 mm, a focal distance of 454 mm, and a ribbed backside construction. The mirror was manufactured by NEC TOSHIBA Space Systems, Ltd. using a reaction sintering method. For more information on the mirror body, refer to [6]. Cryogenic testing on the mirror surface was conducted at the Institute of Space and Astronautical Science of JAXA, and the result obtained is shown in Fig. 2 [7]. This figure shows the difference in mirror accuracy measured when the mirror body was uniformly cooled from 300 to 95 K.

B. Analytical Procedure of Mirror Surface Accuracy

For evaluating the mirror surface, the entire surface of the mirror body was virtually divided into 19 regular hexagons, with the distance between opposite sides being 30 mm (an area of approximately 780 mm² each), on the orthogonal projection of the mirror body, as shown in Fig. 3. From each region, four samples with height 3 mm, width 5 mm, and length 10 mm were cut out in the directions of the cylindrical coordinate system for the entire mirror surface. Two samples were cut in the circumferential

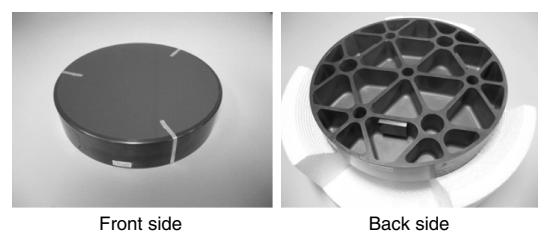


Fig. 1. Appearances of a prototype spherical SiC mirror body examined.

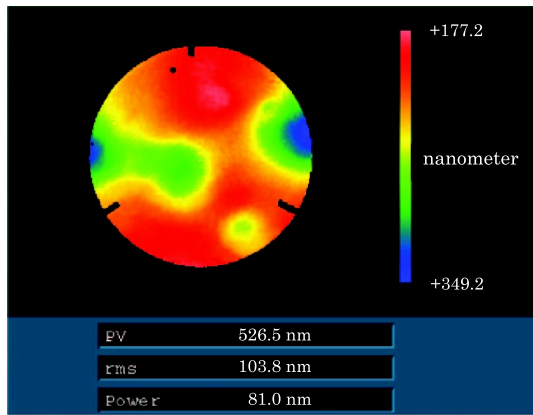


Fig. 2. Result of the cryogenic testing of the mirror body [7]. Temperature: 300 K → 95 K.

longitudinal direction, and the other two were cut in the radial longitudinal direction. The appearance of a sample and the way samples were cut out are shown in Fig. 4. The thermal expansion property and density of the cut-out samples were measured.

The material property of each region was input into the FEM analysis model, and a thermal-structural analysis was carried out by using the commercially available analysis code NEiNastran V9.1 SOL. 101, of NEi Software, Inc. (U.S.), for the case when the entire mirror body was uniformly cooled from 300 to 100 K. The representative spherical surface that best fitted all nodes on the mirror surface obtained after thermal deformation was calculated using the nonlinear least-squares method. The deviations were then calculated, and the distribution of the deviations over the entire mirror surface was obtained in the form of a contour diagram. The analysis evaluation procedure used here is explained in full detail in another paper [5].

C. CTE Measurement and Analysis Based on the Result

The CTE for each sample was measured by the laser interferometry method. For the measurement, we

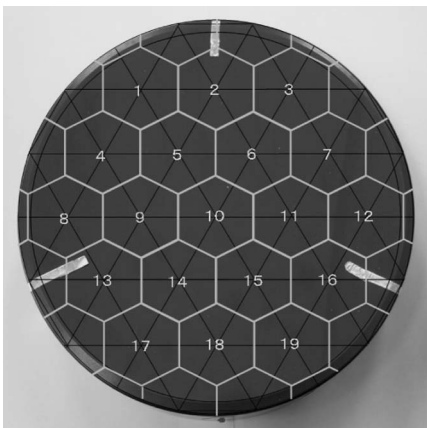


Fig. 3. Orthogonally projected 19 segmented regions on the mirror surface. The regions are regular hexagons with opposite side distances of 30 mm and an area of approximately 780 mm² each.

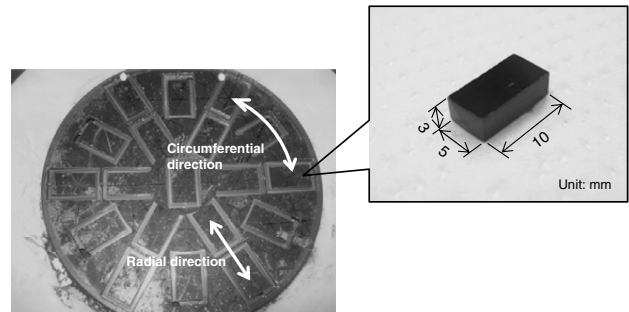


Fig. 4. Appearances of the machining operation for cutting samples out of the mirror body and a cut-out sample (3 mm × 5 mm × 10 mm).

used the laser thermal dilatometer Model LIX-1 of ULVAC Inc. (Japan), which is the most common thermal dilatometer used in Japan. This instrument adopts the dual-path Michelson laser interferometry, based on the absolute measurement method with reference to the wavelength of the laser beam. An interference pattern that moves according to the dimensional change of a specimen is received by an image sensor and measured automatically by a microcomputer by processing the image in real time. The measuring resolution of the dimensional change in a specimen is 2 nm. A preheat-treated sample at 373 K was heated from 123 to 373 K at a constant rate of 2 K/min in helium under a fixed load (about 17 g), and the size change in the longitudinal direction (ΔL) was measured during the process. The lower temperature limit was 123 K, at which the instrument was able to obtain stable data empirically. From ΔL and the initial size (L_0) measured at the room temperature before heating, the temperature-dependent curves of the rate of dimensional change ($\Delta L/L_0$) were obtained.

From the curve and the formulas (1) and (2), the coefficient of linear expansion (α) and the average coefficient of linear expansion ($\bar{\alpha}$) were, respectively, obtained:

$$\alpha = \frac{1}{L_0} \cdot \frac{dL}{dT}, \quad (1)$$

$$\bar{\alpha} = \frac{\left(\frac{\Delta L}{L_0}\right)_{T_1} - \left(\frac{\Delta L}{L_0}\right)_{T_2}}{T_1 - T_2}. \quad (2)$$

Here, α corresponds to the value of the temperature derivative of the temperature-dependent curves of $\Delta L/L_0$, and $\bar{\alpha}$ corresponds to the slope of the straight line passing through temperatures T_1 and T_2 . As ΔT in $\bar{\alpha}$ increases, the accuracy also increases. Note that the α used to input values for analysis was derived by using the central difference method with $dT = 20$ K in order to round the variations at each data point.

In order to reduce error in measurement, the measurement was conducted twice, each with a sample cut out in the circumferential direction and in the

radial direction from each of 19 segmented regions of the mirror surface, and the two measured values were then averaged. The following three types of values were input into each region of the analysis model: (i) the average value of $\bar{\alpha}$ s from 123 to 298 K in the circumferential direction and in the radial direction (one value per region), (ii) $\bar{\alpha}$ s from 123 to 298 K in the circumferential direction and in the radial direction (two values per region), and (iii) α s at every 10 K from 103 to 298 K in the circumferential direction and in the radial direction (two directions and 11 temperature points per region, a total of 22 values). In the analysis for the type (iii) values, 11 computations were successively performed. The values at 123, 113, and 103 K in (iii) were extrapolated linearly from the slope of 123–133 K. The analysis with (i) evaluates the effect of variations in the thermal expansion property that depends on the position on the mirror surface. In addition, with (ii) the effect of directions on the mirror surface, and with (iii) the effect of directions and temperature dependency, respectively, are also considered. The coefficient 10^{-6} for each input value was rounded off to two decimal places to obtain a value of 10^{-8} .

By using these input values, changes in the mirror accuracy due to thermal deformation when the entire mirror body was uniformly cooled from 300 to 100 K were analyzed. The analyses using (i) and (ii) involved one computation each. In the analysis using (iii), the temperature was lowered from 300 to 100 K, 10 K at a time, and computation was performed at each temperature by using the form obtained by the analysis of the previous temperature. The material properties in the direction of thickness of the mirror body, including ribbed construction, were assumed to be fixed. The peripheral area of the mirror surface, outside the 19 segmented regions, was also divided into the same shape, and each of the regions was given the average value of the adjoining regions.

D. Density Measurement and Analysis Based on the Result

By using the dry system automatic density analyzer, AccuPyc 1330-03, which is based on the constant-volume dilatation method (a type of gas displacement technique), of Micromeritics Instrument Corporation (U.S.), the sample volume (V_{samp}) was measured at 298 K in a helium-filled chamber. By using the electronic balance MT5 of Mettler-Toledo International Inc. (U.S.), each sample was weighed at the same temperature to obtain the sample weight (W_{samp}). By using these values, the sample density (ρ) was computed using formula (3), where ρ_a is the air density (0.0012 g/cm³). The nominal accuracy of this measurement was about $\pm 0.5\%$:

$$\rho = \frac{W_{\text{samp}}}{V_{\text{samp}}} + \rho_a. \quad (3)$$

The average measurements of two samples cut out from the same part of the mirror surface in the same direction were defined as the density value

of that part of the mirror surface. At this time, the value with units of grams per cubic centimeter was rounded off to the third decimal place. The circumferential and radial values of the same region were also averaged, and the density value of the region was defined as the average value.

By mapping the magnitude relation of the density values of the regions into the entire mirror surface, between the upper and lower limits of $\bar{\alpha}$ for 123–298 K, the estimated value of the average CTE ($\bar{\alpha}_d$) of the region was obtained. The relative position between the maximum ($\rho_{\text{max.}}$) and the minimum ($\rho_{\text{min.}}$) of the density value of each of the 19 mirror surface regions was interpolated into the range between the maximum ($\bar{\alpha}_{\text{max.}}$) and the minimum ($\bar{\alpha}_{\text{min.}}$) of the average CTE in formula (4). This derived value was defined as the average CTE of each region. The upper and lower limits of the average CTE were derived from the result of the thermal expansion measurement of individual regions that was obtained in advance. However, we assume that such pieces of information will not be available in general when the result of a simpler density measurement is used. Therefore, our aim is to study the appearance of deviations from the ideal mirror surface using available values, such as the existing data of similar materials, manufacturer's catalog values, or values in the literature:

$$\bar{\alpha}_d = \bar{\alpha}_{\text{min.}} \times \frac{\frac{1}{\rho} - \frac{1}{\rho_{\text{max.}}}}{\frac{1}{\rho_{\text{min.}}} - \frac{1}{\rho_{\text{max.}}}} + \bar{\alpha}_{\text{max.}} \times \left(1 - \frac{\frac{1}{\rho} - \frac{1}{\rho_{\text{max.}}}}{\frac{1}{\rho_{\text{min.}}} - \frac{1}{\rho_{\text{max.}}}} \right). \quad (4)$$

By using $\bar{\alpha}_d$ of each region, we analyzed mirror accuracy in the case in which the entire mirror body was uniformly cooled from 300 to 100 K. The analysis conditions were identical to the ones applied when CTE measurement data were used.

3. Results

Examples of temperature-dependent curves of $\Delta L/L_0$ and α obtained from CTE measurement of the cut-out samples are shown in Fig. 5. Measurements were conducted twice each for the two samples cut out in the circumferential direction and the radial direction from one segmented region (region 1 in Fig. 3 in this example), and the data obtained from the four measurements are collectively shown here. $\Delta L/L_0$ increases at an accelerating rate as temperature increases, and based on this behavior, α increases in a way similar to a curve that is slightly convex in the upward direction. The four curves resemble each other over the entire temperature range. Therefore, it appears that stable measurements were conducted.

Such curves were acquired for all 19 segmented regions, and the circumferential and radial $\bar{\alpha}$ in each region and the average over the range of 123–298 K were obtained. The results obtained are summarized in Fig. 6. In order to divide these 19 regions into three

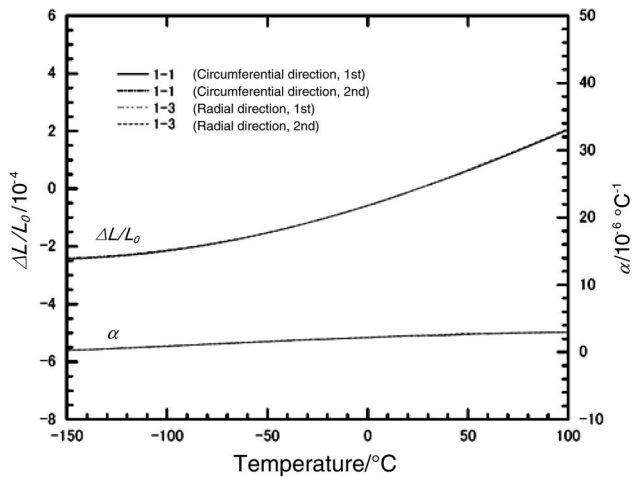


Fig. 5. Examples of temperature-dependent curves of the rate of dimensional change ($\Delta L/L_0$) and the coefficient of linear expansion (α) obtained from thermodilatometry CTE measurement.

groups with an almost equal number of regions per group, boundary values for the averages of $\bar{\alpha}$ were set and the three groups were separately indicated by color coding.

Contour diagrams of the FEM analysis results obtained using the CTE measurement result as input data are shown in Figs. 7(a)–7(c), where the input data used were, as mentioned earlier, (i) the average value of $\bar{\alpha}$ s from 123 to 298 K in the circumferential direction and in the radial direction, (ii) $\bar{\alpha}$ s from 123 to 298 K in the circumferential direction and in the radial direction, and (iii) α s at every 10 K from 103 to 298 K in the circumferential direction and in the radial direction. These contour diagrams show the distribution of deviations of the mirror surface from the representation mirror surface after thermal deformation, which is viewed from the focus of the representation surface. The contour bar values indicate the distances from the focus of the representation mirror surface, based on its radius of curvature.

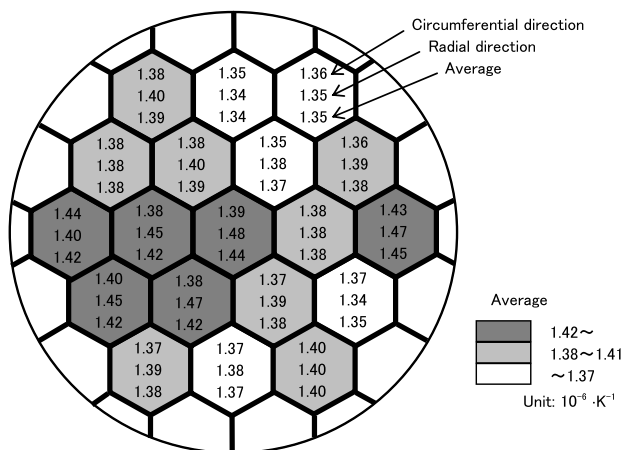


Fig. 6. Results of the average coefficient of linear expansion ($\bar{\alpha}$) over the range of 123–298 K of the 19 segmented regions. The upper, middle, and lower values are the results of the sample of circumferential and radial directions, and those averages, respectively.

Smaller values in warm colors are closer to the focus. In each pair of diagrams (a)–(c), the entire range of deviations occurring on the mirror surface was separated by color in the one on the left, whereas in the one on the right, the range was adjusted and the number of colors was increased so that the diagram would have a very similar appearance to the test result shown in Fig. 2. All the contour diagrams on the right appear similar to the test result, but the contour diagrams to the left of (b) and (c) have a doughnut-shaped rise toward the focus near the center, which was not observed in the test result. Diagram (a), which considered neither directionality nor temperature dependency for the mirror surface, was closest to the test result.

The result of all regions obtained from the density measurement is shown in Fig. 8. Here, 19 regions were divided into three groups with an almost equal number of regions by density value. The estimated value of the average CTE $\bar{\alpha}_d$ computed from the density result is shown in parenthesis in each region.

The contour diagram prepared using $\bar{\alpha}_d$ is shown in Fig. 9. Similar to Fig. 7, in the diagram to the left, the range from the upper to lower limits of the deviations is separated by color, and in the diagram to the right, the range was adjusted arbitrarily. An arc-shaped rise toward the focus on the right side of the center in the left-hand side contour diagram was not in the test result, but the right-hand side contour diagram appeared very similar to the test result as seen in Fig. 7.

Peak to valley (PV) values of individual analyses are summarized in Table 1. While the PV value obtained by a cryogenic testing on the mirror surface was 526 nm, the PV value shown in Fig. 7(a), for which directionality on the mirror surface was not considered, was about 60 nm lower. Conversely, the PV values in Figs. 7(b) and 7(c), for which the directionality on the mirror surface was considered, were 40–50 nm higher. The consideration of temperature dependency did not make a significant difference on these PV values. Incidentally, the PV value obtained from the average CTE value estimated from density measurement data was more than 100 nm lower than the test result.

4. Discussion

As mentioned in Section 1, measuring the mirror surface deviation in orders of several 100 nm occurring at $\Delta T = 200$ K is estimated to require a $10^{-8}/\text{K}$ level measurement accuracy of $\bar{\alpha}$. Since the resolution of the measuring device and the length of the specimen are 2 nm and 10 mm, respectively, we can estimate the measurement accuracy of α to be $\pm 0.2 \times 10^{-6}$ ($2 \text{ nm} \div 10 \text{ mm}$) and the measurement accuracy of $\bar{\alpha}$ at $\Delta T = 200$ K to be $\pm 0.2 \times 10^{-8}/\text{K}$ ($0.2 \times 10^{-6} \times 2 \div 200$). Practically, the accuracy decreases depending on the condition to attach the specimen and the elements of control and measurement of temperature. However, the $10^{-8}/\text{K}$ level accuracy of $\bar{\alpha}$, which

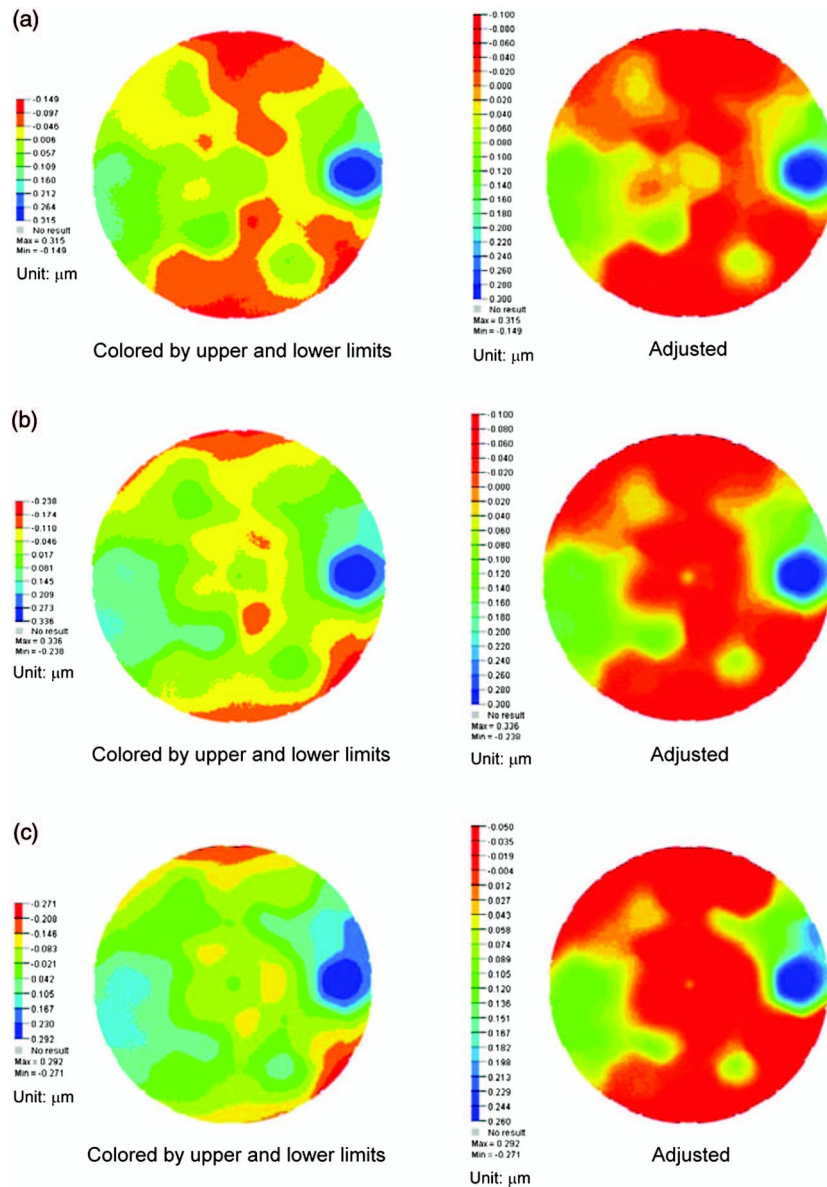


Fig. 7. Contour diagrams of the distributions of deviation of the mirror surface obtained by the FEM analyses using the CTE measurement results: (a) average value of $\bar{\alpha}_s$ at 123–298 K of the two directions, (b) $\bar{\alpha}_s$ at 123–298 K of the two directions, and (c) α_s at every 10 K within 103–298 K of the two directions. Temperature: 300 K \rightarrow 100 K, deviations from the representation mirror surfaces after thermal deformation.

is a digit lower than the estimates, is a realizable range.

All diagrams, Figs. 7(a)–7(c), appeared similar to the test result. Therefore, it is shown that a mirror body manufactured by this method can be used to evaluate the accuracy of the entire mirror surface to some degree, regardless of whether the directionality on the mirror surface and the temperature dependency of the input data of the CTE are considered. Furthermore, among these three, (a) was relatively the closest to the test result compared to (b) and (c). It is thereby suggested that, in the mirror surface accuracy evaluation, it is more effective to obtain several measurements at the same position and then average them to improve the accuracy than to

consider the anisotropy or temperature dependency of material properties separately. It is speculated that, for the thermal expansion property of the base material of this mirror body, there is little or no anisotropy and that the variation in behavior with respect to temperature is also small.

These results are examined from a statistical viewpoint of the samples' CTE measurement results. When the standard deviations of α at every 10 K from 123 to 373 K for all 38 samples (cut out in the circumferential and radial directions in the 19 segmented regions) were determined, they were all found to be in the range of $0.036 - 0.054 \times 10^{-6}/\text{K}$, and the differences were within a very limited range of less than $0.019 \times 10^{-6}/\text{K}$. From these findings, it can be

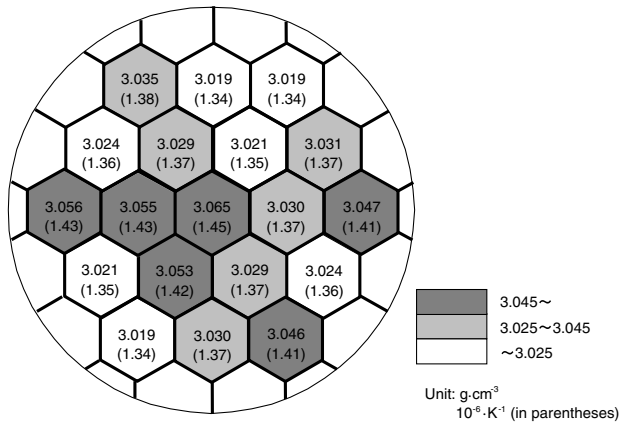


Fig. 8. Results of the density at room temperature of the 19 segmented regions. Values in parentheses are the estimated values of the average CTE from the density measurement result; $\bar{\alpha}_d$.

said that the variation in behavior of the thermal expansion property of this material with respect to temperature is quite small. In addition, while the standard deviation of $\bar{\alpha}$ for the 38 samples at 123–298 K was $0.037 \times 10^{-6}/\text{K}$, the standard deviation for two circumferential and radial samples in each region averaged over 19 regions was $0.023 \times 10^{-6}/\text{K}$, a small value of nearly half, despite the small number of samples. From these findings it can be said that the anisotropy within the mirror surface made of this material is sufficiently small compared to local variations. Furthermore, the

resulting data showed that the standard deviation of α of 38 different samples at the same temperature was within a very small value of less than $0.019 \times 10^{-6}/\text{K}$ and that the CTE variation caused by the difference in the cutting direction at the same position was clearly smaller than the variation caused by the difference in the cutting position. This supports the argument that the accuracy of this measurement satisfied the $10^{-8}/\text{K}$ accuracy level, which is thought to be needed for mirror surface evaluation. This shows that, as speculated in the previous section, the surface evaluation of the mirror body requires little consideration for anisotropy or temperature dependency of material properties, and that most importantly, the data accuracy at the same position needs to be improved.

As seen in Fig. 9, we were able to obtain a result similar to the mirror surface test result by using actual density measurement data. The correlation diagram between the density and the average $\bar{\alpha}$ of circumferential and radial values over the range of 123–298 K at the 19 segmented regions is shown in Fig. 10. Except at a few points, there was a strong correlation between the density and the CTE. The overall coefficient of determination R^2 was 0.6092, and when we removed two points with lower correlativity than others (the points marked with *), R^2 increased to 0.8696. The two points removed were in regions 12 and 13 shown in Fig. 3, and both had high CTE values.

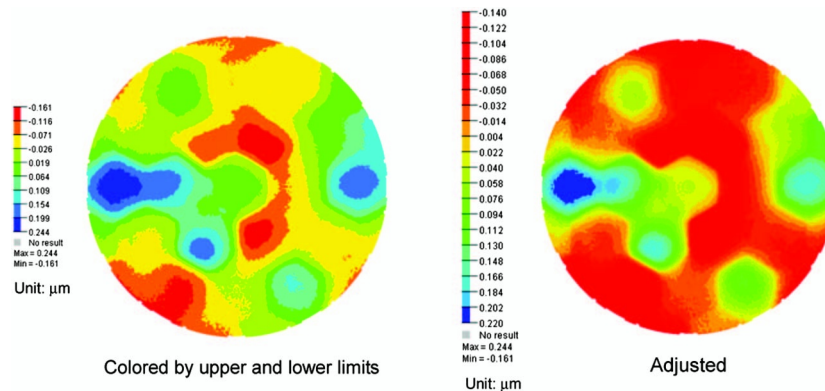


Fig. 9. Contour diagrams of the distribution of deviation of the mirror surface obtained by the FEM analysis using $\bar{\alpha}_d$ values estimated from the density measurement result. Temperature: 300 K \rightarrow 100 K, deviations from the representation mirror surfaces after thermal deformation.

Table 1. Summary of the PV Values Obtained from Various Mirror Surface Evaluations

Related Figure	Evaluation Method	Input Data	Analysis Conditions	PV (nm)
Fig. 2	Mirror surface testing			526
Fig. 7(a)	FEM analysis	CTE measurement data	Neither directionality nor temperature dependency	463
Fig. 7(b)	FEM analysis	CTE measurement data	Only directionality	574
Fig. 7(c)	FEM analysis	CTE measurement data	Both directionality and temperature dependency	563
Fig. 9	FEM analysis	Estimated CTE values from density measurement data	Neither directionality nor temperature dependency	406

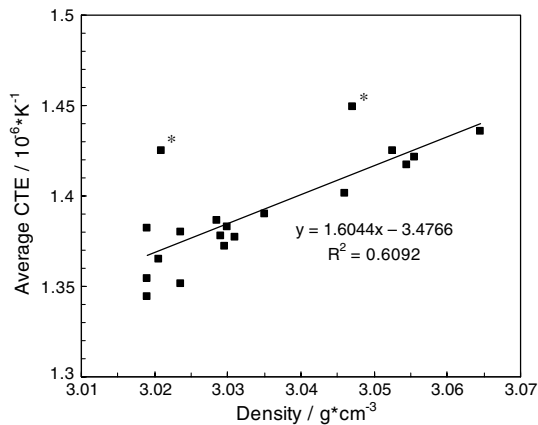


Fig. 10. Correlation diagram between the density at room temperature and the average $\bar{\alpha}$ of circumferential and radial values at 123–298 K for the 19 segmented regions.

It would appear that, among the factors that affect the density of this mirror body material, there exists a microstructural factor that affects the thermal expansion property. According to a paper published by the manufacturer [8], in this material, all carbon sources existing in the green body before reaction sintering became SiC by sintering and all voids were filled with melted Si. This material contains microstructures wherein unreacted Si is distributed like islands in the SiC phase. Therefore, the density is mainly affected by the content percentage of unreacted Si, and as the percentages of Si (specific gravity of 2.3 g/cm³), which has lower specific gravity than SiC (3.2 g/cm³), increase, the density decreases. As the density decreases, the CTE also decreases, as shown in Fig. 10, which means that as the percentages of Si increase, the CTE decreases. The CTEs of the material of this mirror body, obtained as the average of 38 samples, are $1.39 \times 10^{-6}/\text{K}$ at 120 K, $1.92 \times 10^{-6}/\text{K}$ at 200 K and $2.42 \times 10^{-6}/\text{K}$ at 300 K. However, there is a report about Si [9] that gives lower values of $-6.0 \times 10^{-8}/\text{K}$ at 120 K, $1.4 \times 10^{-6}/\text{K}$ at 200 K, and $2.62 \times 10^{-6}/\text{K}$ at 300 K, and hence, this tendency seems to follow the law of mixture for the CTE of material constituents.

The errors in the PV values between the analyses using the CTE test results and the mirror surface test were around 50 nm, which is a relatively small value considering the numerical error of the analysis (about 30 nm according to our prior examination). Compared to the case in which the directionality on the mirror surface was not considered, the PV values were larger when the directionality was considered, and we speculate that the reason is simply that there were many different types of CTE input values. PV value error factors include, in addition to CTE measurement error, representation of material properties, which are continuously distributed over the entire mirror body by a limited number of samples, a slight difference in temperature conditions between the mirror surface testing (300 K \rightarrow 95 K) and the analysis (300 K \rightarrow 100 K), and the use of $\bar{\alpha}$

obtained at 123–298 K for the analysis in this temperature range. Despite various error factors such as these, it can be said that the accuracy values were successfully reproduced.

5. Conclusion

We investigated a technology for evaluating mirror accuracy in the case of thermal deformation of a SiC mirror body by FEM analysis, which used the actual measurement data of the material properties. Major results obtained from the study are listed below.

1. We demonstrated that the appearance of the mirror surface deviation and the PV values can be evaluated to an accuracy of around 50 nm with the obtained data from the samples cut out from various positions on the mirror surface at about 30 mm intervals.

2. We verified that, without considering CTE properties, such as the cutting direction on the mirror surface, temperature dependency, and ribbed construction, we can achieve, to a certain degree, high accuracy for this mirror body material.

3. We demonstrated that, for the mirror body material, we can evaluate the appearance of the mirror surface deviation accurately to a certain degree by using density data alone, which can be more easily obtained than CTE data.

The authors acknowledge the support provided by Mr. Yoshikazu Muta of Tokyo University of Science for examinations in the early stage of the study, and by JAXA staff members Ms. Rei Ueda and Mr. Kenichi Tomoda, for processing of the analysis data. We also acknowledge the support provided by Mr. Soichi Takeda and Mr. Keisuke Arafurue of Digital Solutions Inc. in various aspects of mirror accuracy analysis, and by Toray Research Center, Inc. for CTE and density measurements. We take this opportunity to express our gratitude for all your support and guidance.

References

1. T. Nakagawa, H. Matsuhara, and Y. Kawakatsu, "The next-generation infrared space telescope SPICA," *Proc. SPIE* **8442**, 844200 (2012).
2. R. Edeson, G. S. Aglietti, and A. R. L. Tatnall, "Conventional stable structures for space optics: the state of the art," *Acta Astronaut.* **66**, 13–32 (2010).
3. J. Breyse, D. Castel, B. Laviro, D. Logut, and M. Bougoin, "All-SiC telescope technology: recent progress and achievements," in *Proceedings of the 5th International Conference on Space Optics (ICSO 2004)*, B. Warmbein, ed., (2004), pp. 659–671.
4. E. Sein, Y. Toulemon, J. Breyse, P. Deny, D. de Chambure, T. Nakagawa, and M. Hirabayashi, "A new generation of large SiC telescopes for space applications," *Proc. SPIE* **5528**, 83–95 (2004).
5. M. Kotani, T. Imai, H. Katayama, Y. Yui, Y. Tange, H. Kaneda, T. Nakagawa, and K. Enya, "Quality evaluation of spaceborne SiC mirrors (I): analytical examination of the effects on mirror accuracy by variation in the thermal expansion property of the mirror surface," *Appl. Opt.* **52**, 4797–4805 (2013).
6. K. Tsuno, H. Irikado, K. Oono, J. Ishida, S. Suyama, Y. Itoh, N. Ebizuka, H. Eto, Y. Dai, W. Lin, T. Suzuki, H. Omori, Y. Y. Yui,

- T. Kimura, and Y. Tange, "New-technology silicon carbide (NT-SiC): demonstration of new material for large lightweight optical mirror," Proc. SPIE **5659**, 138–145 (2005).
7. H. Kaneda, T. Nakagawa, T. Onaka, K. Enya, H. Kataza, S. Makiuti, H. Matsuhara, M. Miyamoto, H. Murakami, H. Saruwatari, H. Watarai, and Y. Y. Yui, "Development of lightweight SiC mirrors for the space infrared telescope for cosmology and astrophysics (SPICA) mission," Proc. SPIE **6666**, 666607 (2007).
8. S. Suyama, Y. Itoh, A. Kohyama, and Y. Katoh, "Development of high strength reaction-sintered silicon carbide," J. Ceram. Soc. Jpn. **109**, 315–321 (2001).
9. G. K. White and M. L. Minges, "Thermophysical properties of some key solids," Int. J. Thermophys. **18**, 1269–1327 (1997).